

FEDSM-ICNMM2010-30559

PRESSURE DROP IN MICROCHANNELS FILLED WITH POROUS MEDIA

A. Tamayol

Multiscale Thermofluidic Laboratory for
Sustainable Energy Research,
School of Engineering Science,
Simon Fraser University, BC, Canada
ali_tamayol@sfu.ca

B. Gray

MicroInstrumentation Laboratory,
School of Engineering Science,
Simon Fraser University, BC, Canada
bgray@sfu.ca

A. Khosla

MicroInstrumentation Laboratory,
School of Engineering Science,
Simon Fraser University, BC, Canada
ajit_khosla@sfu.ca

M. Bahrami

Multiscale Thermofluidic Laboratory for
Sustainable Energy Research,
School of Engineering Science,
Simon Fraser University, BC, Canada
mbahrami@sfu.ca

Abstract

The pressure drop in microchannels filled with porous media formed by square arrays of cylinders (micro-porous channels) is investigated. Combining the Brinkman equation and the existing models for permeability of regular arrays of cylinders, the pressure drop in the considered micro-porous channels is calculated theoretically. Soft lithography method is used to fabricate several Polydimethylsiloxane (PDMS) microporous-channels with porosities in the range of 0.35 to 0.95, fiber diameters varying from 50 to 400 μm , and channel depth of approximately 100 μm . Distilled water is pushed through the samples using a syringe pump with steady flow rate and the resulting pressure drops are measured for several flow rates. The theoretical model captures the trends of experimental data for all of the samples. Our analysis indicates that a competing behaviour exists between the permeability and the channels dimensions for controlling the pressure drop. Therefore, the Darcy number should be used to determine the dominating parameter.

1 Introduction

Microchannels offer high heat and mass transfer coefficients, high surface to volume ratio, and low thermal resistance. As such, they have been utilized in applications such as electronics cooling, aerospace, MEMS, medical and biomedical devices [1-3]. The major drawback in using microchannels is the dramatic increase of pressure drop which is inversely proportional to the cross-sectional length scale [4]. To alleviate this problem, the channels cross-sectional size should be increased which reduces the surface to volume ratio of the designed chip. However, one solution is to combine mini/microchannels with porous media to develop a novel design. Similar to microchannels, highly porous structures feature low-weight, high surface-to-volume ratios, and high heat transfer coefficients [5]. Therefore, it is expected that microchannels filled with porous media (micro-porous channels) have thermal properties similar to that of regular microchannels while the pressure drop is lower. Micro-porous channels also have potential applications in filtration, detection of particles, and

tissue engineering [6]. Moreover such structures have been used in biological and life sciences for analyzing biological materials such as proteins, DNA, cells, embryos, and chemical reagents [7,8]. Although the fully developed and developing flows in channels of various cross-sections filled with porous media have been extensively studied in the literature, see for example [9-11], such studies for micron size channels are not numerous. Recently, Hooman and his coworkers [12,13] have investigated rarefied gas flows in microchannels filled with porous media. But, their theoretical analyses were not verified by any experimental data.

Few experimental studies have been conducted to study flow through mini/microchannels filled with micro pin fins. Kosar et al. [14] studied laminar flow across four different arrays of micro pin fins embedded inside in microchannels with 100 μm depth. Pin fins diameter in their study were 50 and 100 μm . They compared their results for Reynolds numbers in the range of 5-128 with existing correlations for relatively high Reynolds number flows through macro-scale tube banks and observed a significant deviation. Kosar et al. [14] related this deviation to difference between flow in micro and regular-size systems. Vanapalli et al. [15] measured pressure in microchannels of 250 μm depth containing various pillar arrays in the Reynolds number range of 50-500. On the contrary, their results for circular pillars were in good agreement with conventional relationships. Yeom et al. [16] reported low Reynolds number flow pressure drops through micro-porous channel with various fibers in square arrangements. The channels were 200 μm deep and the diameters of the microposts ranged from 200 μm to less than 10 μm . Yeom et al. [16] did not include wall effects in their analysis. As a result, their data for high permeability arrays deviated from the values predicted by conventional theories.

To the best knowledge of the authors, there is no study of pressure drop in micro-porous channels and comparison of the data with the theories developed for regular size porous channels. As such, the goals of this study are to:

- Employ the theoretical studies developed for regular size channels for predicting the pressure drop of liquid flows through microchannels filled with porous media.

- Perform an independent experimental study to verify the theoretical analysis.
- Determine the importance of different parameters such as permeability and cross-sectional geometry on the pressure drop in the investigated microsystems.

In this study, the porous medium is represented by several square arrangements of cylinders. Employing the Brinkman model for confined porous media and the analytical model developed by Tamayol and Bahrami [17] for permeability of square arrangement of fibers, pressure drop in the considered geometries is calculated theoretically. In addition, water flow pressure drops are measured in several PDMS micro-porous channels with different cylinder sizes and porosities. The developed model is successfully compared with the measured data.

2 Theoretical Background

The micro-porous channel, shown in Fig. 1, is assumed to be comprised of repeating square arrangements of mono disperse cylinders, embedded in a rectangular microchannel. Several researchers have stated that in creeping flow regime, the fully developed condition is achieved within the first 3 columns of cylinders; see for example [18]. Therefore, the entrance effects are neglected in this study. As such, fully developed, steady state, incompressible, and creeping flows of a Newtonian fluid inside micro-porous channels is studied.

In low Reynolds number flows, a linear relationship is assumed between the applied pressure drop and the volume averaged velocity which is called the Darcy equation:

$$\frac{dP}{dz} = -\frac{\mu}{K}U \quad (1)$$

where, μ is the fluid viscosity and K is the permeability of the medium. The Darcy relationship is empirical, convenient, and widely accepted. However, when the boundary effects become significant, the Brinkman equation [19] should be used:

$$\frac{dP}{dz} = -\frac{\mu}{K}U + \mu_{eff} \frac{d^2U}{dy^2} \quad (2)$$

where μ_{eff} is called the effective viscosity. Previous studies have shown that the viscosity ratio, $\hat{\mu} = \mu_{eff}/\mu$, varies between 1 to ~ 10 [20]. However, for simplicity, in the present study the effective viscosity is considered to be identical to the dynamic viscosity,

μ . This assumption is reasonable for highly porous materials [21]. The last term in the right hand side of Eq. (2) has been originally added to the Darcy equation to enable the solution to fulfill the no-slip boundary condition on solid walls. In the limiting case where either there is no porous medium inside the channel or the boundary effects are dominant, Darcy term, the first term in the right hand side of Eq. (2), vanishes and this equation becomes identical to Navier-Stokes (NS) equation. On the other hand, in the limit of very dense porous media, the Darcy term becomes dominant and Eq. (2) reduces to Eq. (1).

Hooman and Merrikh [22] have developed analytical solutions for flow and pressure drop inside large scale rectangular channels filled with porous:

$$\frac{\Delta P}{L} = \frac{\mu Q}{Wh^3} \frac{1}{2 \sum_{n=1}^{\infty} \frac{1}{\lambda_n^2 m^2} \left(1 - \frac{\tanh m \varepsilon'}{m \varepsilon'}\right)} \quad (3)$$

where

$$\varepsilon' = \frac{h}{W}, \quad \lambda_n = \frac{(2n-1)\pi}{2}, \quad s = \frac{h}{\sqrt{K}}, \quad (4)$$

$$m = (\lambda_n^2 + s^2)^{1/2}$$

and h , L , and W are the depth, length, and width of the porous channel, respectively.

The cross-sectional aspect ratio, ε' , in the samples tested in the present study is smaller than 0.1.

Therefore, instead of considering the whole rectangular cross-section, the channel can be modeled as a porous medium sandwiched between two parallel plates. The pressure drop for the simplified geometry is determined and simplified as:

$$\frac{\Delta P}{L} = \frac{\mu Q \sinh\left(\frac{h}{\sqrt{K}}\right)}{Kh \left[2 \frac{\sqrt{K}}{h} \left[-1 + \cosh\left(\frac{h}{\sqrt{K}}\right) \right] - \sinh\left(\frac{h}{\sqrt{K}}\right) \right]} \quad (5)$$

To further investigate the accuracy of this assumption, the relative difference between the solutions of the 2D problem and the model of Hooman and Merrikh [22], Eq. (3), is plotted in Fig. 2. It can be seen that the relative difference is less than %8 for low aspect ratio micro-porous channels. Since Eq. (5) is more compact than Eq. (3), this equation is used in the present study.

To calculate the pressure drop from either Eq. (3) or Eq. (5), one needs to know the permeability of the fibers arrangement in the normal directions which is discussed in the following subsection.

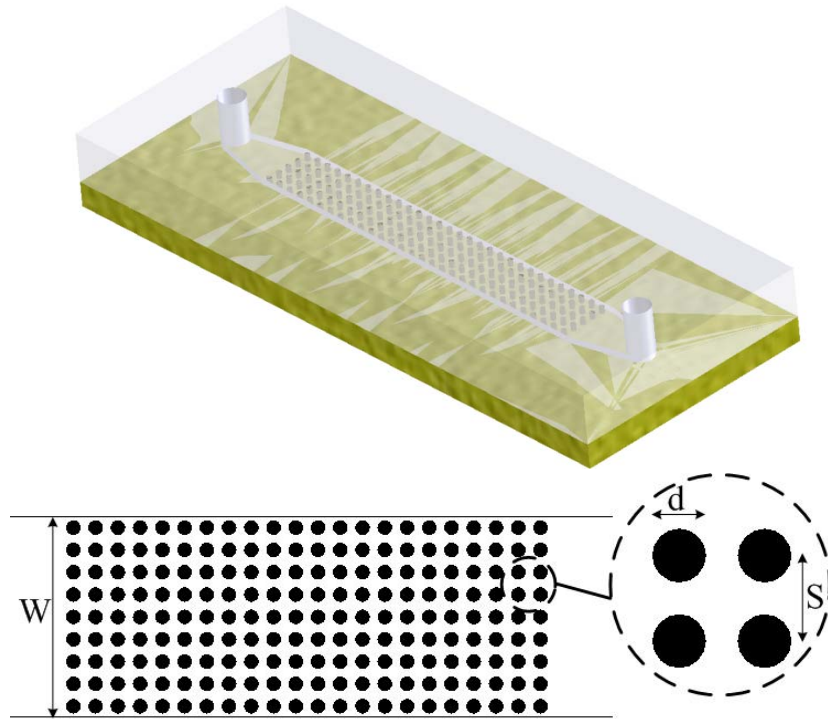


Figure 1: Schematic of the considered micro-porous channels.

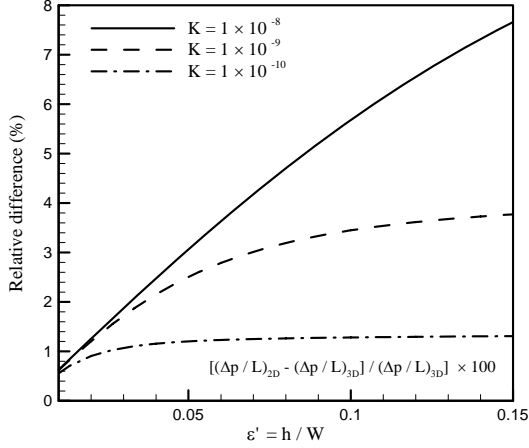


Figure 2: Relative difference between Eqs. (3) and (5).

2-1 Permeability of the cylinders array

The normal permeability of ordered cylinders has been studied extensively in the literature [17, 23-29]. Recently, Tamayol and Bahrami [17] have employed an integral technique solution to develop analytical models for permeability of square arrangement of fibers. The porosity for these arrangements is determined from:

$$\varepsilon = 1 - \frac{\pi d^2}{4S^2} \quad (6)$$

where S is the distance between adjacent cylinders and d is the diameter of the cylinders. The following relationship was reported for the permeability of square arrangement of fibers [17]:

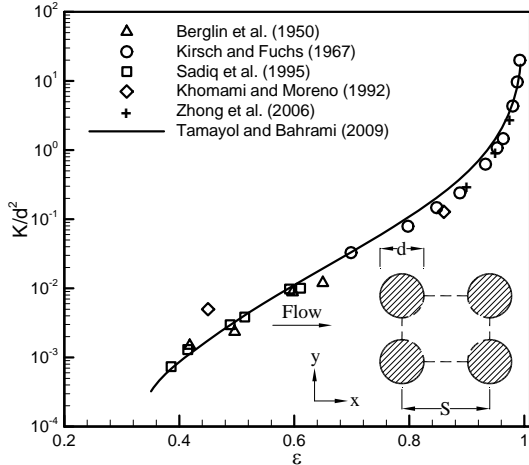


Figure 3: Comparison of Eq. (7) with experimental data for normal permeability of square arrangement of fibers [14].

$$K^* = \left\{ \frac{12(\sqrt{\varphi'} - 1) \left[\frac{2 - g(\varepsilon)}{2} \right]}{\varphi' \sqrt{\varphi'}} + \frac{18 + 12(\varphi' - 1)}{\sqrt{\varphi'}(1 - \varphi')^2} + \frac{27\pi\sqrt{\varphi'}}{2(\varphi' - 1)^{\frac{5}{2}}} \right\}^{-1} \quad (7)$$

where $K^* = K/d^2$, $\varphi' = \pi/4(1 - \varepsilon)$ and $g(\varepsilon) = 1.274\varepsilon - 0.274$. Equation (7) is compared with experimental data for normal permeability of unidirectional fibers [18,30-33] in Fig. 3. It can be seen that the model of [17] is in a reasonable agreement with experimental data over the entire range of porosity. As such, Eq. (7) is used to calculate permeability of the cylinders located inside the microchannels.

3 Experimental procedure

3.1 Microfabrication

The PDMS/PDMS microchannels used in this study have been manufactured using the soft lithography technique [34] described by Erickson et al. [35]. A schematic of the process is provided in Fig. 4. The fabrication process has two main parts: 1) preparing the mold; 2) making the PDMS replica.

SU-8 was used for preparing the molds; SU-8 is a negative tone epoxy-based photoresist that can be photo patterned using deep UV light. SU-8-100 was chosen for micromold fabrication as it can be patterned in very thick films (up to 1mm thick or more) and makes an excellent mold for PDMS. Square glass slides of 75 x 75 mm and 1mm thick were used as substrates which were first cleaned in 100% Micro 90 Detergent (purchased from International Products Corporation, USA) using ultrasonic agitation for 5 minutes and then rinsed with de-ionized (DI) water, acetone, isopropyl alcohol (IPA) and DI water. Substrates were blow dried using nitrogen followed by dehydration baking for 20 minutes at 120°C in a convection oven and cooling to room temperature. A 25 nm thick chrome layer was sputtered on each glass substrate which acts as an adhesion promoter for the SU-8 100. A 100 μm thick layer of SU-8 100 was spin coated (at 2250 RPM) on top of the adhesion layer of each substrate, followed by soft baking at 90 °C for 80 minutes and cooling to room temperature. Structures were patterned using photolithographic UV exposure through a photomask for 60 seconds. Full crosslinking of the SU-8 100 was achieved by a post-exposure bake at a temperature of 60°C for 65

minutes (ramp rate: 300 °C/hr) followed by cooling to room temperature. The structural layer on each substrate was then developed in SU-8 Developer (Microchem™) for 90 seconds in an ultrasonic bath. Liquid PDMS was then poured over the mold and trapped bubbles were extracted by placing the liquid PDMS inside a vacuum chamber for 1h. The replica was then cured at 85°C for 45 minutes yielding a negative cast of the microchannel pattern. An enclosed microchannel was then formed by bonding the PDMS cast with another piece of PDMS via plasma treatment. The fabrication steps are depicted in Fig. 4.

Five different samples were fabricated and tested in the present study. As a result of the fabrication uncertainty the sizes of the channels and the cylinders were different from their intended dimensions. To measure the actual sizes, an image processing technique was employed. In this approach, images of the channel were taken using a high CCD camera (Hamanatsu Orca AG, NJ) under microscope. Dimensions of features were estimated by counting the number of pixels between two points. Accuracy of this method was reported by Akbari et al. [36] to be 3.6 μm.

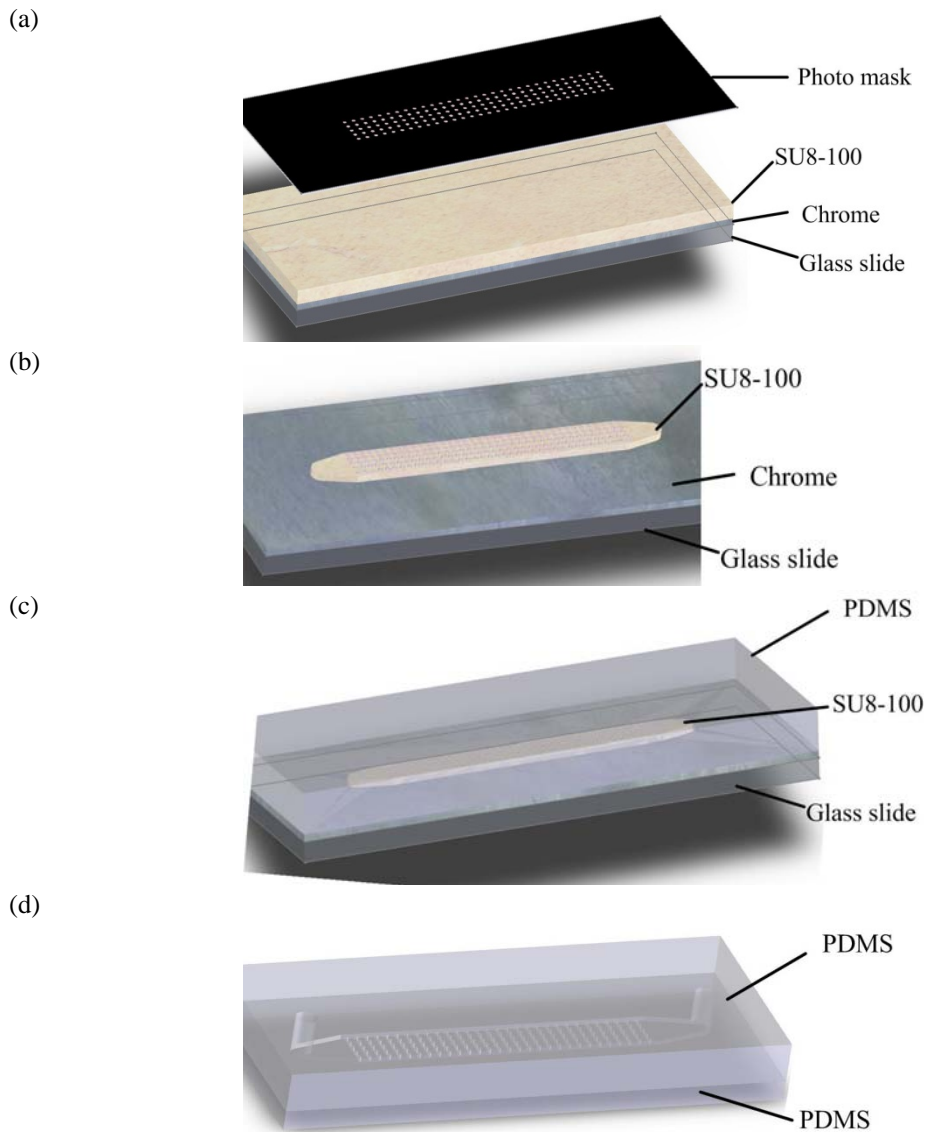


Figure 4: Fabrication process steps for SU-8 micromold preparation via photopatterning of SU-8 100 epoxy-based photopolymer: a) spin coating SU-8 100, b) photopatterning and making the mold, c) pouring liquid PDMS, and d) plasma bonding and making the channels.

Table 1: Geometrical properties of the fabricated samples.

Channel	d (μm)	S (μm)	ε	K (m^2)	W (mm)	h (μm)	L (cm)
Sq-0.40-400 (1)	426	456	0.32	1.85×10^{-11}	3.18	96	1.46
Sq-0.40-400 (2)	418	456	0.34	3.30×10^{-11}	3.19	105	1.46
Sq-0.70-100	92	162.1	0.75	3.93×10^{-10}	1.45	105	1.72
Sq-0.90-50	52	129	0.89	6.89×10^{-10}	1.27	129	2.00
Sq-0.95-50	54	118	0.94	2.49×10^{-9}	1.70	118	2.22

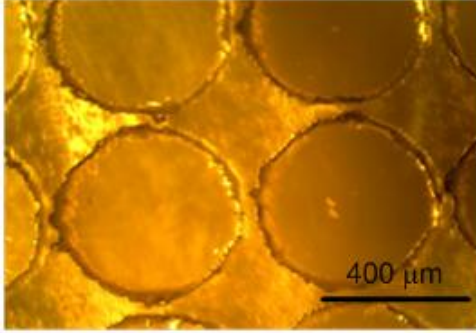


Figure 5: Rough surface of the fabricated cylinders, Sq 04-400 (1).

Our images reveal that the surfaces of the fabricated cylinders were rough, see Fig. 5. As such, for determining the cylinders sizes, diameters of ten different cylinders were measured in three different directions for each sample and the average of these thirty values was considered as the size of the cylinders. In order to measure the width and the depth, the samples were cut at three random locations. The cutting lines were perpendicular to the channel to ensure a 90 deg viewing angle. The average of the measured values was considered as the actual size of the channels. The geometrical properties of the sample are summarized in Table 1. The channels' names in the table indicate the cylinder arrangement, intended porosity, and the expected cylinders diameter, e.g., Sq-0.40-400 corresponds to square arrangement of 400 μm cylinders with porosity of 0.4. In addition, the permeabilities of the embedded porous media, calculated from Eq. (7), are reported in Table 1.

3.2 Test setup

The open loop system, illustrated in Fig. 6, was employed for measuring the steady pressure drop in the fabricated samples of micro-porous channels. A syringe pump (Harvard Apparatus, QC, Canada) was feeding the system with a controlled flow rate with

0.5% accuracy. Water was forced to flow through a submicron filter before entering the channel. To measure the pressure drop, a gauge pressure transducer with 1% accuracy (Omega Inc., Laval, QC, Canada) was fixed at the channel inlet while the channel outlet was discharged to the atmosphere. Teflon tubing (Scientific Products and Equipment, North York, Canada) was employed to connect the pressure transducer to the syringe pump and the microchannel. Pressure drops were measured for several flow rates in the range of 50-800 $\mu\text{l}/\text{min}$.

4 Analysis of experimental data

Viscous dissipations effect is neglected in this study; thus, the properties of the flowing water are considered to be constant. The measured pressure drop during the experiment, ΔP_{total} , is:

$$\Delta P_{total} = \Delta P_c + \Delta P_D + \Delta P_{FD} + \Delta P_{minor} + \Delta P_{ev} \quad (8)$$

where ΔP_c is the pressure loss in the connecting tubes between the pressure transducer and the sample inlet, see Fig. 6, ΔP_D is the pressure drop in the developing region of the samples where the fully-developed flow is not achieved, ΔP_{FD} is the pressure drop in the regions with fully-developed velocity distribution. ΔP_{minor} is the pressure drop due to minor losses in the samples including 90 deg bends in the inlet and outlet of the samples, and ΔP_{ev} is the pressure drop corresponding to the electroviscous effect [37]. Akbari et al. [36] showed that ΔP_{minor} and ΔP_{ev} are less than 1% of the ΔP_{FD} and can be neglected.

The connecting pressure loss, ΔP_c , is measured directly at each flow rate when the end of the tubing is disconnected from the sample. To perform accurate measurements, the level of the tubing end should be identical to the case where the samples are connected; this avoids from any error due to hydrostatic pressure difference.

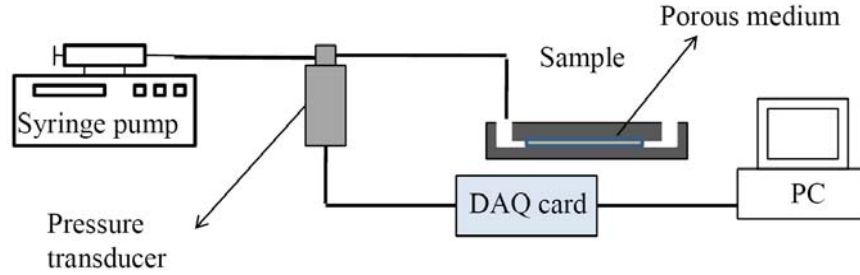


Figure 6: Schematics of the designed experimental setup.

The developing length in the micro-porous samples depends on the channel size and the permeability of the porous medium embedded inside. For highly permeable porous structures, the flow-field is very similar to plain channel flows while for fiber arrays with low permeability, the volume-averaged velocity distribution is significantly affected by the fibers and is analogous to Darcy flow, see Fig. 7. For the former case, as a result of low Reynolds numbers, the viscous boundary layer grows very fast in microchannels. As shown by Akbari et al. [36] the developing pressure drop in microchannels is less than 1% of the total pressure loss and is negligible. For the case of pack fibers, fully-developed condition is achieved in the first three rows [18]. Therefore, the measured pressure drop in the sample is considered to that of the fully-developed flows presented by Eqs. (3) or (5).

5 Comparison of the model with the experimental data

Figures 8 and 9 show the measured values of pressure drop of the micro-porous channels versus the volumetric flow rate. The flow rates are selected such that the pressure drop in the channels is higher than the accuracy of the pressure transducer. It can be seen that the trends of the experimental data are well predicted by the theoretical results. The deviations of most of the measured values from theoretical predictions are less than 10%. The deviations are more intense for Sq-0.9-50 (Max 15%); this is caused by the inaccuracy in the channels cross-section measurements which has a significant impact on the predicted pressure drops. The $\pm 10\%$ region for theoretical predictions are shown in Fig. 9.

The experimental values of pressure drop have a linear relationship with volumetric flow rate. It can be argued that the channels were not deformed during the experiment otherwise a nonlinear trend would be observed in the experimental data; for detailed

discussions see [38]. Moreover, the linear trend of the experimental data shows that the minor losses and the inertial effects are insignificant in the tested microchannels. It should be noted that the maximum Reynolds number based on cylinders' diameter is less than 5; this, justifies the observed trends in the measured values.

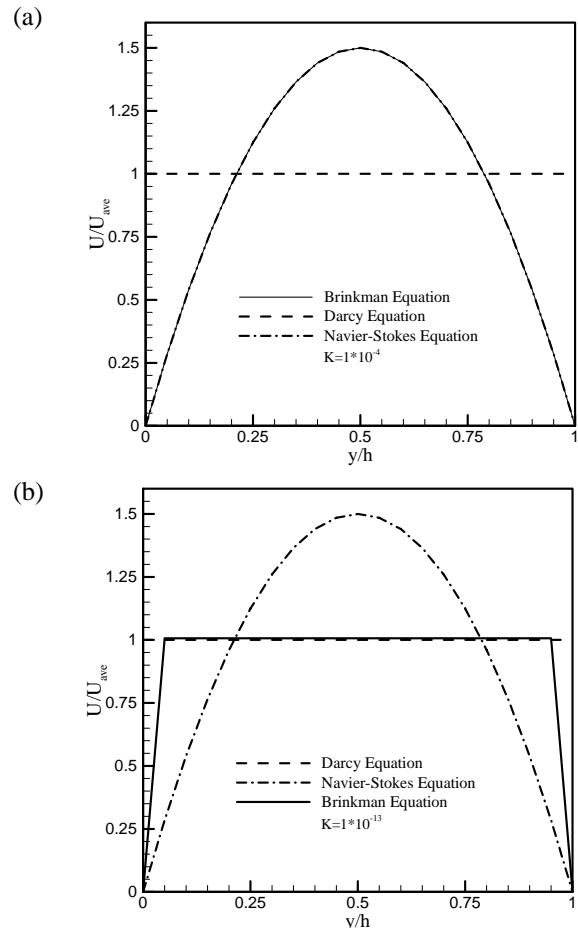


Figure 7: Comparison of velocity distributions predicted by Brinkman equation with the results of Darcy and Navier-Stokes equations, a) highly permeable, b) low permeability porous media.

In the present micro-porous channels, two parameters affect the pressure drop: 1) the permeability, K ; 2) the channel depth, h . To investigate the effect of these parameters, the dimensionless pressure drop is plotted versus the Darcy number in Fig. 10. According to Nield and Kuznetsov [39] and Tamayol et al. [40], the hydrodynamic boundary layer thickness scales with \sqrt{K} . As such, the Darcy number, K/h^2 can be interpreted as the ratio of the boundary layer thickness to the depth of the channel. Figure 10 shows that Eq. (5) is in reasonable agreement with the experimental data. In addition, it can be seen that Eq. (5) has two asymptotes. First, for micro-porous channels with very dilute porous medium, low Darcy number, the pressure drop can be predicted by solving the Navier-Stokes equation for plain channels. Second, for channels with very packed porous medium, high Darcy numbers, Eq. (5) predicts the same results as the Darcy law. As such, one can conclude that the Darcy number can be used for determining the controlling parameter in the pressure drop in micro-porous channels.

6 Summary and conclusions

Pressure drop in micro-porous channels with porous structure comprised of straight cylinders in ordered arrangements was studied. The Brinkman equation was used to predict the overall pressure drop, where permeability of the porous medium was evaluated from the model proposed by Tamayol and Bahrami [20] for the permeability of square arrangement of fibers.

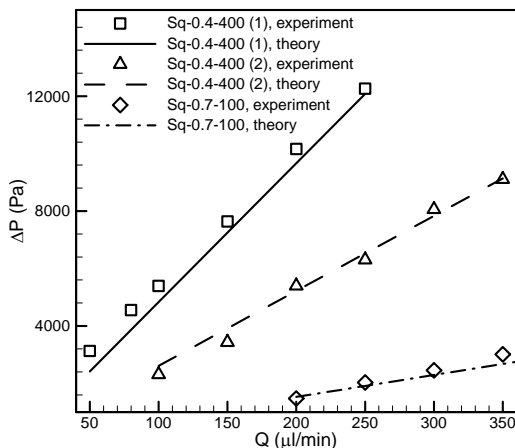


Figure 8: Channel pressure drop versus flow rate for Sq-0.4-400 (1), Sq-0.4-400 (2), and Sq-0.7-100. Lines show the theoretical values of pressure drop using Eq. (5) and symbols show the experimental data.

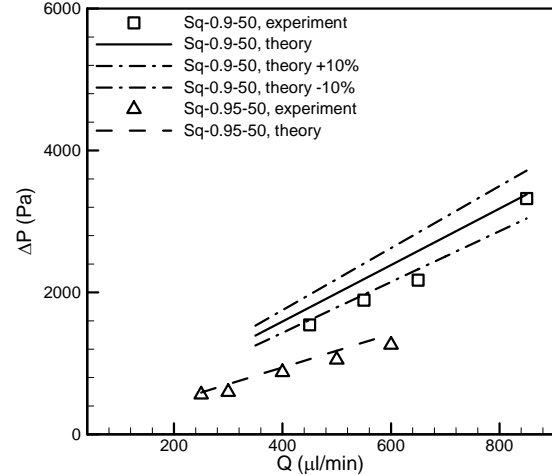


Figure 9: Channel pressure drop versus flow rate for Sq-0.9-50 and Sq-0.95-50. Lines show the theoretical values of pressure drop using Eq. (5) and symbols show the experimental data.

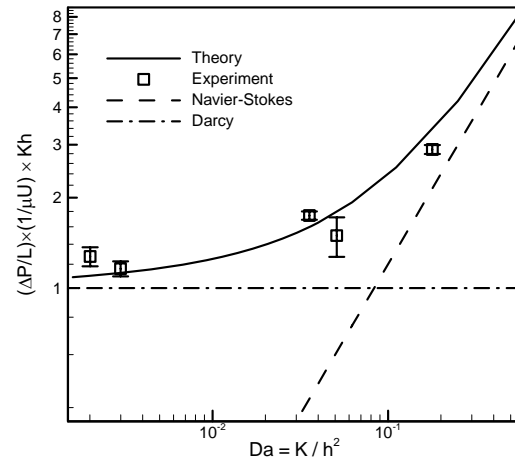


Figure 10: Dimensionless pressure drop versus Darcy number.

To verify the theoretical analysis, soft lithography method was used to fabricate five PDMS micro-porous channels with porosity in the range of 0.33 to 0.95, fiber diameter from 50 to 400 μm , approximately 100 μm deep. Water was pushed through the samples and the overall pressure drop was measured for different flow rates. The theoretical model was successfully compared with experimental data. Our analysis suggested that the Darcy number was the dimensionless number that determines the controlling parameters in the pressure drop. For high Darcy numbers, the channel dimensions played a major role in the overall pressure drop while in low Darcy numbers the cylinders geometry and permeability were the controlling parameters in determining the pressure drop.

7 Acknowledgements

The authors gratefully acknowledge the financial support of the Natural Sciences and Engineering Research Council of Canada (NSERC).

8 References

[1] D.B. Tuckerman, R.F. Pease, 1981, "High-performance heat sinking for VLSI," *IEEE Electron Device Letters*, Vol. 5, pp. 126–129.

[2] M. Bahrami, A. Tamayol, P. Taheri, 2009, "Slip-flow pressure drop in microchannels of general cross-section," *ASME Journal of Fluid Engineering*, Vol. 131, pp. 1036-1044.

[3] G.M. Whitesides, 2006, "The origins and the future of microfluidics," *Nature (London)*, Vol. 442, pp. 368–372.

[4] D. Pence, 2008, "The simplicity of fractal-like flow networks for effective heat and mass transport," *ECI International Conference on Heat Transfer and Fluid Flow in Microscale*, Whistler, Canada.

[5] L. Tadrist, M. Miscevic, O. Rahli, F. Topin, 2004, "About the use of fibrous materials in compact heat exchangers," *Experimental Thermal and Fluid Science*, Vol. 28, pp. 193–199.

[6] P.R. Waghmare, S.K. Mithra, A. Mather, J. McLaughlin, 2008, "Modeling, fabrication and simulation of microfilters," *ECI International Conference on Heat Transfer and Fluid Flow in Microscale*, Whistler, Canada.

[7] C. Yu, M.H. Davey, F. Svec, J.M.J. Fréchet, 2001, "Monolithic porous polymer for on-chip solid-phase extraction and preconcentration prepared by photoinitiated in situ polymerization within a microfluidic device," *Analytical Chemistry*, Vol. 73, pp. 5088–5096.

[8] D.J. Throckmorton, T.J. Shepodd, A.K. Singh, 2002, "Electrochromatography in microchips: reversed-phase separation of peptides and amino acids using photopatterned rigid polymer monoliths," *Analytical Chemistry*, Vol. 74, pp. 784-789.

[9] A. Haji-Sheikh, 2006, "Fully developed heat transfer to fluid flow in rectangular passages filled with porous materials," *ASME Journal of Heat Transfer*, Vol. 128, pp. 550–556.

[10] A. Haji-Sheikh, W.J. Minkowycz, E.M. Sparrow, 2004, "Green's function solution of temperature field for flow in porous passages," *International Journal of Heat and Mass Transfer*, Vol. 47, pp. 4685–4695.

[11] D.A. Nield, A.V. Kuznetsov, M. Xiong, 2003, "Thermally developing forced convection in a porous medium: parallel plate channel with walls at uniform temperature, with axial conduction and viscous dissipation effects," *International Journal of Heat and Mass Transfer*, Vol. 46, pp. 643–651.

[12] K. Hooman, 2008, "A superposition approach to study slip-flow forced convection in straight microchannels of uniform but arbitrary cross-section," *International Journal of Heat and Mass Transfer*, Vol. 51, pp. 3753-3762.

[13] K. Hooman, 2008, "Heat transfer and entropy generation for forced convection through a microduct of rectangular cross-section: effects of velocity slip, temperature jump, and duct geometry," *International Communications in Heat and Mass Transfer*, Vol. 35, pp. 1065–1068.

[14] A. Kosar, C. Mishra, Y. Peles, 2005, "Laminar flow across a bank of low aspect ratio micro pin fins," *Journal of Fluids Engineering*, Vol. 127, pp. 419-430.

[15] S. Vanapalli, H.J.M. Ter Brake, H.V. Jansen, J.F. Burger, H.J. Holland, T.T. Veenstra, M.C. Elwenspoek, 2007, "Pressure drop of laminar gas flows in a microchannel containing various pillar matrices," *Journal of Micromechanics and Microengineering*, Vol. 17, pp. 1381.

[16] J. Yeom, D.D. Agonafer, J.H. Han, M.A. Shannon, 2009, "Low Reynolds number flow across an array of cylindrical microposts in a microchannel and figure-of-merit analysis of micropost-filled microreactors," *Journal of Micromechanics and Microengineering*, Vol. 19, 065025.

[17] A. Tamayol, M. Bahrami, 2009, "Analytical determination of viscous permeability of fibrous porous media," *International Journal of Heat Mass Transfer*, Vol. 52, pp. 3691-3701.

[18] W.H. Zhong, I.G. Currie, D.F. James, 2006, "Creeping flow through a model fibrous porous medium," *Experiments in Fluids*, Vol. 40, pp. 119-126.

[19] H. Brinkman, 1949, "A calculation of the viscous force exerted by a flowing fluid on a dense swarm of particles," *Applied Science Research*, Vol. A1, pp. 27-34.

[20] R.C. Givler, S.A. Altobelli, 1994, "A determination of the effective viscosity for the Brinkman-Forchheimer flow model," *Journal of Fluid Mechanics*, Vol. 258, pp. 355-370.

[21] V.M. Starov, V.G. Zhdanov, 2001, "Effective viscosity and permeability of porous media," *Colloids Surfaces A*, Vol. 192, pp. 363–375.

[22] K. Hooman, A.A. Merrikh, 2006, "Analytical solution of forced convection in a duct of rectangular cross section saturated by a porous medium," *ASME Journal of Heat Transfer*, Vol. 128, pp. 596-600.

[23] S. Kuwabara, 1959, "The forces experienced by randomly distributed parallel circular cylinders or spheres in a viscous flow at small Reynolds numbers," *Journal of Physical Society of Japan*, Vol. 14, pp. 527-532.

- [24] H. Hasimoto, 1959, "On the periodic fundamental solutions of the stokes equations and their application to viscous flow past a cubic array of spheres," *Journal of Fluid Mechanics*, Vol. 5, pp. 317–328.
- [25] J. Happel, 1959, "Viscous flow relative to arrays of cylinders," *AICHE*, Vol. 5, pp. 174–177.
- [26] J.E. Drummond, M.I. Tahir, 1984, "Laminar viscous flow through regular arrays of parallel solid cylinders," *International Journal of Multiphase Flow*, Vol. 10, 515-540.
- [27] M. Sahraoui, M. Kaviani, 1994, "Slip and no-slip boundary condition at interface of porous, plain media," *International Journal of Heat Mass Transfer*, Vol. 37, pp. 1029–1044.
- [28] A. S. Sangani, A. Acrivos, Slow Flow Past Periodic Arrays of Cylinders with Application to Heat Transfer, *International Journal of Multiphase Flow*, Vol. 8, pp.193–206, 1982.
- [29] A. Tamayol, M. Bahrami, 2010, "Transverse permeability of fibrous porous media," *Third International Conference on Porous Media and its Applications in Science, Engineering and Industry*, Montecatini, Italy.
- [30] O.P. Bergelin, G.A. Brown, H.L. Hull, F.W. Sullivan, 1950, "Heat transfer and fluid friction during viscous flow across banks of tubes: III – a study of tube spacing and tube size," *ASME Transactions*, Vol. 72, pp. 881–888.
- [31] A. A. Kirsch, N.A. Fuchs, 1967, "Studies on fibrous aerosol filters—II pressure drops in systems of parallel cylinders," *Annals of Occupational Hygiene*, Vol. 10, pp. 23–30.
- [32] T. A. K. Sadiq, S. G. Advani, R. S. Parnas, 1995, "Experimental investigation of transverse flow through aligned cylinders," *International Journal of Multiphase Flow*, Vol. 21 (5), pp. 755–774.
- [33] B. Khomami and L. D. Moreno, 1997, "Stability of viscoelastic flow around periodic arrays of cylinders," *Rheologica. Acta*, Vol. 36 (4), pp. 367–383.
- [34] J.C. McDonald, D.C. Duffy, J.R. Anderson, D.T. Chiu, H. Wu, O.J.A. Schueller, G. Whiteside, 2000, "Fabrication of microfluidic systems in poly(dimethylsiloxane), *Electrophoresis*," Vol. 21, pp. 27–40.
- [35] D. Erickson, D. Sinton, D. Li, 2003, "Joule heating and heat transfer in poly(dimethylsiloxane) microfluidic systems," *Lab on a Chip*, Vol. 3, pp. 141–149.
- [36] M. Akbari, M. Bahrami, D. Sinton, 2009, "Flow in rectangular microchannels: an experimental investigation," *ASME Journal Fluid Engineering*, Vol. 131, pp. 041203-1-10.
- [37] R.F. Probstein, 1994, "Physicochemical hydrodynamics," 2nd ed., Wiley, New York.
- [38] M.A. Holden, S. Kumar, A. Beskok, P.S. Cremer, 2003, "Microfluidic diffusion diluter: bulging of PDMS Microchannels under pressure driven flow," *Journal of Micromechanics and Microengineering*, Vol. 13, pp. 412–418.
- [39] D.A. Nield, A.V. Kuznetsov, 2005, "Forced convection in porous media: transverse heterogeneity effects and thermal development," In: Vafai, K., (ed.) *Handbook of Porous Media*, 2nd ed., pp. 143-193. Taylor and Francis, New York.
- [40] A. Tamayol, K. Hooman, M. Bahrami, 2010, "Thermal analysis of flow in a porous medium over a permeable stretching wall," *Transport in Porous Media*, In Press.